

Long-term observation of Markarian 501 by LHAASO-WCDA

Dixuan Xiao,^{a,*} Shuwang Cui,^a Min Zha,^{b,c} Bing Zhang^{c,d} and Shilong Chen^{c,d,e}
on behalf of LHAASO Collaboration

^aHebei Normal University,
050024 Shijiazhuang, Hebei, China

^bKey Laboratory of Particle Astrophysics & Experimental Physics Division & Computing Center, Institute
of High Energy Physics, Chinese Academy of Sciences,
100049 Beijing, China

^cTIANFU Cosmic Ray Research Center,
610213 Chengdu, Sichuan, China

^dKey Laboratory of Particle Astrophysics and Experimental Physics Division and Computing Center,
Institute of High Energy Physics, Chinese Academy of Sciences,
100049 Beijing, China

^eLaboratory for Relativistic Astrophysics, Department of Physics, Guangxi University,
530004 Nanning, China

E-mail: xiao_dixuan@163.com, zham@ihep.ac.cn, zhangbing@ihep.ac.cn

Based on 42 months of observations by the Large High Altitude Air Shower Observatory (LHAASO), we report on the active behavior of the blazar Mrk 501, which exhibited several high states during this period. The most dramatic flare occurred between MJD 59334 and MJD 59348, reaching 62% of the Crab Nebula flux (> 1 TeV). The global spectral energy distribution (SED) of Mrk 501 above 1 TeV is well described by a power-law model with an exponential cutoff, yielding a power-law index of $\alpha = 2.18 \pm 0.04$ and a cutoff energy of $E_{\text{cut}} = 9.51 \pm 1.44$ TeV. Ongoing studies focus on multi-wavelength correlations and broadband spectral modeling to further understand the underlying physical mechanisms driving these phenomena. LHAASO's all-weather capability and high duty cycle provide critical continuous data for such investigations.

39th International Cosmic Ray Conference (ICRC2025)
15–24 July 2025
Geneva, Switzerland



*Speaker

1. Introduction

Blazars constitute a type of Active Galactic Nuclei (AGN) characterized by relativistic jets oriented along our line of sight. Markarian 501 (Mrk 501), classified as a BL Lacertae blazars, is a powerful extragalactic source of Very High Energy (VHE) gamma rays, first detected by the Whipple (10-meter gamma-ray) telescope [1]. Notably, Mrk 501 exhibits significant variability across multiple energy bands. In 1997, the source entered an exceptionally high state, reaching a luminosity approximately six times that of the Crab Nebula, accompanied by a hard spectral index of 2.46 [2]. This dramatic flaring activity was not only observed in the VHE gamma-ray band but also prominently detected in X-rays. Observations from the *Rossi X-Ray Timing Explorer* (RXTE) [3] revealed that the X-ray emission during this event displayed highly variable behavior, with the synchrotron component extending up to energies of 100 keV. According to Synchrotron Self-Compton (SSC) models, gamma-ray emission originating from leptonic processes is expected to exhibit a strong correlation with X-ray emission. Consequently, long-term, unbiased multi-wavelength observations are essential for understanding the underlying physical mechanisms. The Large High Altitude Air Shower Observatory (LHAASO), with its high sensitivity and high duty cycle, is uniquely positioned to provide critical insights into the VHE gamma-ray behavior of such sources.

2. Experiment

The Large High Altitude Air Shower Observatory (LHAASO), situated at Haizi Mountain (29°21′27.56″N, 100°08′19.66″E, 4410 meters above sea level) in Sichuan Province, China, is a hybrid Extensive Air Shower (EAS) detector array. It comprises three main components: a 1.3 km² array (KM2A), a water Cherenkov detector array (WCDA), and a wide field-of-view air Cherenkov telescope array (WFCTA).

The WCDA consists of three water ponds covering a total area of 78,000 m² and is equipped with 3,120 water Cherenkov detectors (WCDs). Each detector is fitted with photomultiplier tubes (PMTs) of two sizes: 8-inch and 1.5-inch PMTs for the first pond, and 20-inch and 3-inch PMTs for the other two ponds. Simulations indicate that the energy threshold of the WCDA reaches 100 GeV. Further details have been published in [4–6]. The WCDA is characterized by its all-weather detection capability, wide field-of-view, and high sensitivity, achieving a duty cycle exceeding 98% and monitoring approximately 1/7 of the sky daily through transit observations. Consequently, the WCDA provides unbiased and continuous data without interruption.

The KM2A array is composed of 5,195 electromagnetic detectors (EDs) and 1,188 muon detectors (MDs), deployed over an area of 1.3 km². The EDs are spaced at intervals of 15 m, while the MDs are spaced at intervals of 30 m. A typical ED has a detection efficiency of approximately 98% and a time resolution of about 2 ns. The MDs are pure water Cherenkov detectors, shielded by 2.5 meters of soil. A typical MD has a detection efficiency exceeding 95% and a time resolution of about 10 ns. Additional details have been published in [5, 7, 8].

3. Results

Figure 1 presents the 42-month multi-wavelength light curves spanning from March 2021 to July 2024. In the VHE regime, Mrk 501 exhibited significant variability, indicating active gamma-ray emission, while no substantial outbursts were observed in the 0.1 - 100 GeV and 15 - 50 keV bands. Several notable peaks and piled-up outbursts are evident. A particularly prominent burst occurred between MJD 59337 and MJD 59348, during which the flux rapidly increased. A similar structure was observed in both the LAT and XRT observations. Another distinctive feature was a long-term elevated state of Mrk 501, lasting from MJD 59400 to MJD 59800. This period began with an overall increase in flux, followed by several outbursts at the peak, and concluded with a gradual decline in flux, described as an "exhaustion" phase. This phenomenon is more pronounced in the XRT observations. Following the elevated state, Mrk 501 entered a quiescent phase, with the majority of data points clustering in the lower flux range, interspersed with occasional spikes.

3.1 Global Spectra of Energy Distribution

By accumulating data over extended periods, LHAASO can provide a comprehensive picture of Active Galactic Nuclei (AGN) behavior, including variations in luminosity and spectral characteristics. This continuous dataset enables the investigation of long-term evolution and facilitates studies based on uninterrupted, no-alarm data.

Given that LHAASO's measurements extend to several TeV, the attenuation due to pair production induced by the low-energy extragalactic background light (EBL) has a non-negligible effect on the observed flux. To derive the intrinsic spectral model of Mrk 501, we assumed both a power-law model and a power-law model with an exponential cutoff:

$$F = F_0 \left(\frac{E}{1 \text{ TeV}} \right)^{-\alpha}, \quad (1)$$

$$F = F_0 \left(\frac{E}{1 \text{ TeV}} \right)^{-\alpha} \exp \left(-\frac{E}{E_{\text{cut}}} \right), \quad (2)$$

which were convolved with EBL models [15–17]. The corrected SEDs, along with the observed SED (without EBL correction), are shown in Figure 2. The intrinsic spectrum of Mrk 501 exhibits a curvature around 10 TeV, which cannot be adequately explained by a simple power-law model. Instead, a power-law model with an exponential cutoff is preferred. The best-fit parameters are $F_0 = 10.89 \pm 0.31 \times 10^{-12} \text{ TeV}^{-1} \cdot \text{cm}^{-2} \cdot \text{s}^{-1}$, $\alpha = 2.18 \pm 0.04$, and $E_{\text{cut}} = 9.51 \pm 1.44 \text{ TeV}$, with minimal variation across the three EBL models considered.

we compare LHAASO's results to spectra measured by other instruments (MAGIC[18]; VERITAS [18]; HAWC[19]; ARGO-YBJ[20] and TACTIC[21]) in Figure 3.

3.2 Flaring Behavior

During the observation period, Mrk 501 exhibited several flaring, with the most dramatic flare occurring in the interval MJD 59334 and MJD 59348 (see Figure 4). To characterize the timescales of these flares, we employed an exponential function with asymmetric rise (T_r) and decay (T_d) timescales:

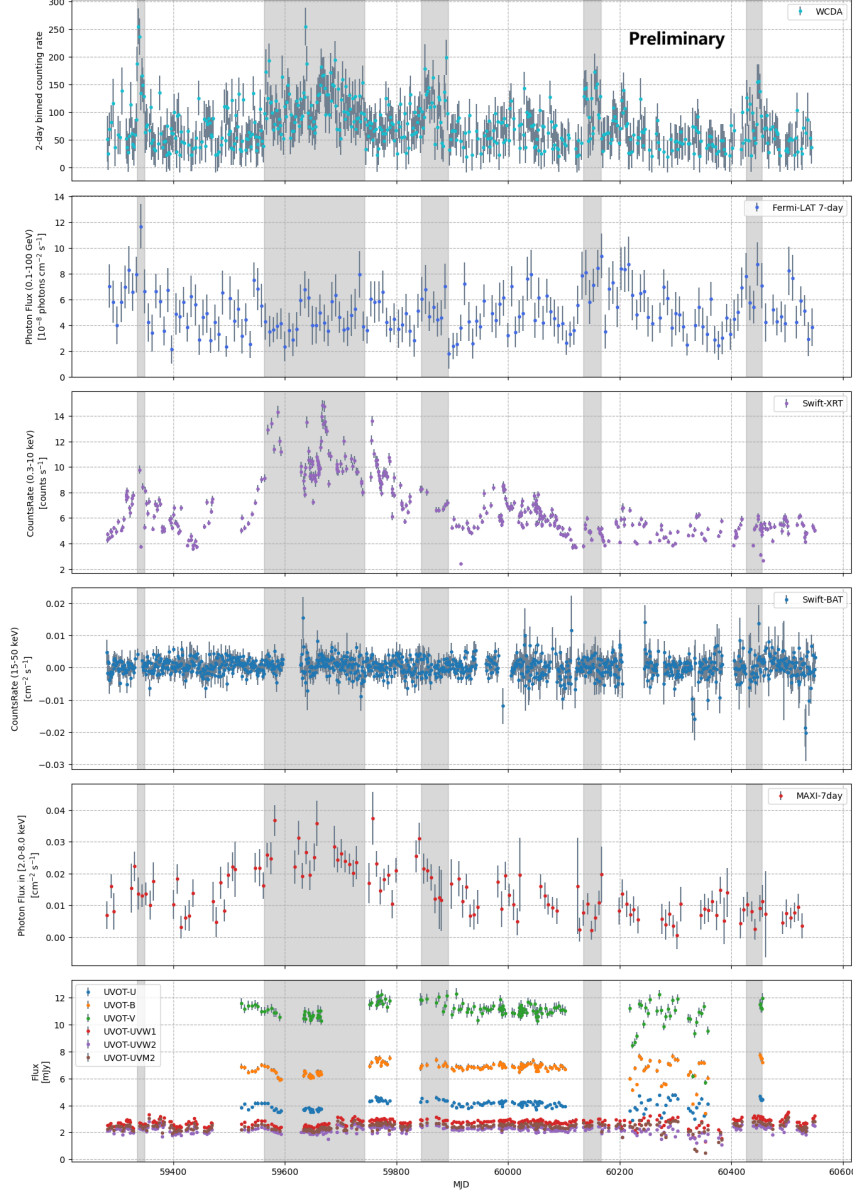


Figure 1: Long term Mrk501 multi-wavelength light curves spanning from 59281 until end of 60550. Top to bottom: WCDA 2-day binned counting rate for $N_{hit} > 60$; Fermi-LAT 3-day fluxes for energy $\in [0.1, 100]$ GeV from Fermi Light Curve Repository (LCR)[9, 10]; Swift-XRT X-ray counting rate for energy $\in [0.3, 10]$ keV from UK Swift Science Data Centre (UKSSDC)[11, 12]; Swift-BAT hard X-ray counting rate for energy $\in [15, 50]$ keV from Swift/BAT Hard X-ray Transient Monitor[13]; MAXI X-ray 7-day binned counting rate for energy $\in [2, 8]$ keV from MAXI on-demand process[14] and Swift-UVOT fluxes of six filters from UKSSDC. Grey shadow regions denote the high states depended on LHAASO-WCDA observation.

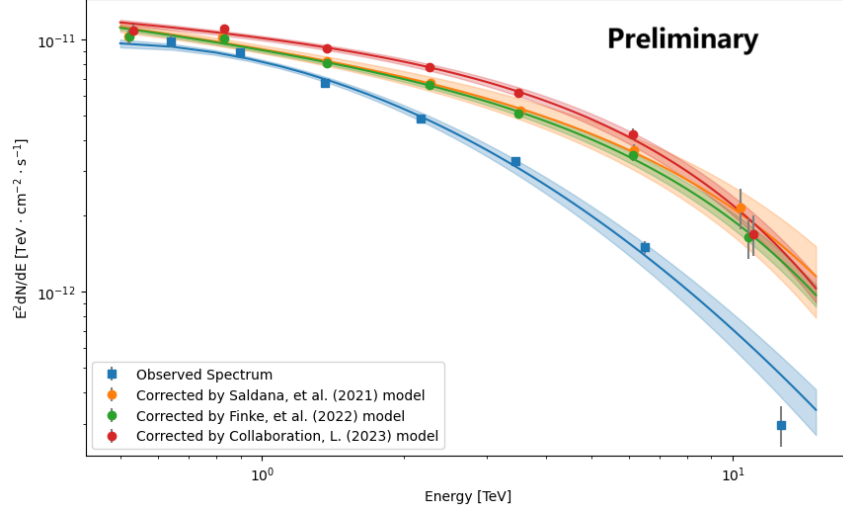


Figure 2: The spectral models after EBL correction. Colored shaded region means 1σ uncertainty of fitting.

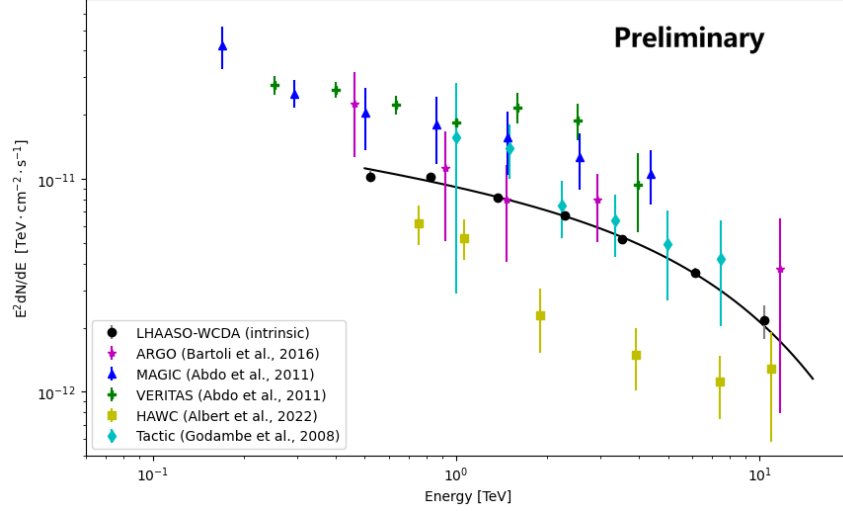


Figure 3: Comparison with previous results. MAGIC (16.2 hr) and VERITAS (9.7 hr) from [18], HAWC (1038 days) from [19], ARGO-YBJ experiment between 2007 and 2010 from [20] and TACTIC telescope (129.25 hr) from [21].

$$F(t) = 2F_v \left[\exp\left(\frac{t_0 - t}{T_r}\right) + \exp\left(\frac{t - t_0}{T_d}\right) \right]^{-1} + F_c \quad (3)$$

where t_0 represents the peak time, F_c is the constant baseline counting rate, and F_v is the flaring component superimposed on the baseline rate. The parameter T_r corresponds to the rise timescale and T_d to decay timescale.

During this flare, the brightness of Mrk 501 increased by a factor of 6 relative to its quiescent state within 2 days, rising from 9% to 62% of the Crab Nebula flux (> 1 TeV), and subsequently decayed over the course of 6 days. The asymmetric timescales of the flare, characterized by a shorter

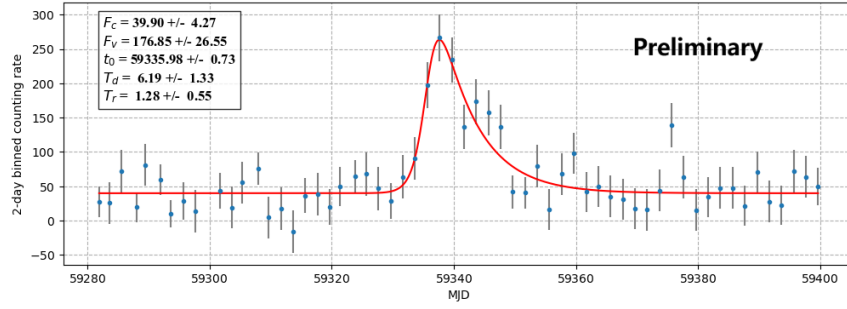


Figure 4: Detail light curve in the beginning and toward the end of the time range (MJD 59274 to MJD 59407). The blue data points represent the measured 2-day binned counting rate, with error bars indicating the uncertainties. A red line overlays the data, representing a fitted model.

rise time and a longer decay time, may indicate that the particle acceleration process occurs more rapidly than the cooling process. The underlying physical mechanisms driving this phenomenon remain under investigation.

4. Summary

Based on 42 months of observations conducted by LHAASO, we find that Mrk 501 exhibits relatively active behavior, experiencing several high states. The most dramatic flare occurred during MJD 59334 and MJD 59348, reaching 62% of the Crab Nebula flux (> 1 TeV). The global SED of Mrk 501 above 1 TeV is well described by a power-law model with an exponential cutoff, characterized by a power-law index of $\alpha = 2.18 \pm 0.04$ and a cutoff energy of $E_{\text{cut}} = 9.51 \pm 1.44$ TeV. Studies on multi-wavelength correlations and broadband spectral modeling are currently ongoing.

Acknowledgments

We would like to thank all staff members who work at the LHAASO site above 4400 meter above the sea level year-round to maintain the detector and keep the water recycling system, electricity power supply and other components of the experiment operating smoothly. We are grateful to Chengdu Management Committee of Tianfu New Area for the constant financial support for research with LHAASO data. We appreciate the computing and data service support provided by the National High Energy Physics Data Center for the data analysis in this paper. This work is supported by the following grants: the National Natural Science Foundation of China nos. 12393853, 12393851, 12393852, 12393854.

References

- [1] J. Quinn, C. Akerlof, S. Biller, J. Buckley, D. Carter-Lewis, M.F. Cawley et al., *Detection of gamma rays with $e > 300$ gev from markarian 501*, *The Astrophysical Journal* **456** (1996) L83.

- [2] HEGRA-Collaboration, *Measurement of the flux, spectrum, and variability of tev gamma-rays from mkn 501 during a state of high activity*, *Arxiv preprint astro-ph/9706019* (1997) .
- [3] P. Uttley, I. McHardy and I. Papadakis, *Measuring the broad-band power spectra of active galactic nuclei with rxte*, *Monthly Notices of the Royal Astronomical Society* **332** (2002) 231.
- [4] F. Aharonian, Q. An, L. Bai, Y. Bai, Y. Bao, D. Bastieri et al., *Performance of lhaaso-wcda and observation of the crab nebula as a standard candle*, *Chinese Physics C* **45** (2021) 085002.
- [5] X.-H. Ma, Y.-J. Bi, Z. Cao, M.-J. Chen, S.-Z. Chen, Y.-D. Cheng et al., *Chapter 1 lhaaso instruments and detector technology **, *Chinese Physics C* **46** (2022) 030001.
- [6] Z. Cao, F. Aharonian, Q. An, Y. Bai, Y. Bao, D. Bastieri et al., *The first lhaaso catalog of gamma-ray sources*, *The Astrophysical Journal Supplement Series* **271** (2024) 25.
- [7] Z. Cao, F.A. Aharonian, Q. An, Axikegu, L.X. Bai, Y.X. Bai et al., *Ultrahigh-energy photons up to 1.4 petaelectronvolts from 12 gamma-ray galactic sources*, *Nature* **594** (2021) 33.
- [8] F. Aharonian, Q. An, L. Bai, Y. Bai, Y. Bao, D. Bastieri et al., *Observation of the crab nebula with lhaaso-km2a- a performance study*, *Chinese Physics C* **45** (2021) 025002.
- [9] W. Atwood, A.A. Abdo, M. Ackermann, W. Althouse, B. Anderson, M. Axelsson et al., *The large area telescope on the fermi gamma-ray space telescope mission*, *The Astrophysical Journal* **697** (2009) 1071.
- [10] M. Ackermann, M. Ajello, A. Albert, A. Allafort, W. Atwood, M. Axelsson et al., *The fermi large area telescope on orbit: event classification, instrument response functions, and calibration*, *The Astrophysical Journal Supplement Series* **203** (2012) 4.
- [11] P. Evans, A.P. Beardmore, K.L. Page, L. Tyler, J.P. Osborne, M.R. Goad et al., *An online repository of swift/xrt light curves of-ray bursts*, *Astronomy & Astrophysics* **469** (2007) 379.
- [12] P. Evans, A. Beardmore, K. Page, J. Osborne, P. O'Brien, R. Willingale et al., *Methods and results of an automatic analysis of a complete sample of swift-xrt observations of grbs*, *Monthly Notices of the Royal Astronomical Society* **397** (2009) 1177.
- [13] H.A. Krimm, S.T. Holland, R.H. Corbet, A.B. Pearlman, P. Romano, J.A. Kennea et al., *The swift/bat hard x-ray transient monitor*, *The Astrophysical Journal Supplement Series* **209** (2013) 14.
- [14] M. Matsuoka, K. Kawasaki, S. Ueno, H. Tomida, M. Kohama, M. Suzuki et al., *The maxi mission on the iss: science and instruments for monitoring all-sky x-ray images*, *Publications of the Astronomical Society of Japan* **61** (2009) 999.
- [15] A. Saldana-Lopez, A. Domínguez, P.G. Pérez-González, J. Finke, M. Ajello, J.R. Primack et al., *An observational determination of the evolving extragalactic background light from the*

- multiwavelength hst/candels survey in the fermi and cta era, Monthly Notices of the Royal Astronomical Society* **507** (2021) 5144.
- [16] J.D. Finke, M. Ajello, A. Domínguez, A. Desai, D.H. Hartmann, V.S. Paliya et al., *Modeling the extragalactic background light and the cosmic star formation history, The Astrophysical Journal* **941** (2022) 33.
- [17] L. Collaboration, *A tera-electronvolt afterglow from a narrow jet in an extremely bright gamma-ray burst 221009a, arXiv preprint arXiv:2306.06372* (2023) .
- [18] A. Abdo, M. Ackermann, M. Ajello, A. Allafort, L. Baldini, J. Ballet et al., *Insights into the high-energy γ -ray emission of markarian 501 from extensive multifrequency observations in the fermi era, The Astrophysical Journal* **727** (2011) 129.
- [19] A. Albert, R. Alfaro, C. Alvarez, J.A. Camacho, J. Arteaga-Velázquez, K. Arunbabu et al., *Long-term spectra of the blazars mrk 421 and mrk 501 at tev energies seen by hawc, The Astrophysical Journal* **929** (2022) 125.
- [20] B. Bartoli, P. Bernardini, X. Bi, Z. Cao, S. Catalanotti, S. Chen et al., *4.5 years of multi-wavelength observations of mrk 421 during the argo-ybj and fermi common operation time, The Astrophysical Journal Supplement Series* **222** (2016) 6.
- [21] S. Godambe, R. Rannot, P. Chandra, K. Yadav, A. Tickoo, K. Venugopal et al., *Very high energy γ -ray observations of mrk 501 using the tactic imaging γ -ray telescope during 2005–06, Journal of Physics G: Nuclear and Particle Physics* **35** (2008) 065202.

A. The LHAASO Collaboration

Zhen Cao^{1,2,3}, F. Aharonian^{3,4,5,6}, Y.X. Bai^{1,3}, Y.W. Bao⁷, D. Bastieri⁸, X.J. Bi^{1,2,3}, Y.J. Bi^{1,3}, W. Bian⁷, A.V. Bukevich⁹, C.M. Cai¹⁰, W.Y. Cao⁴, Zhe Cao^{11,4}, J. Chang¹², J.F. Chang^{1,3,11}, A.M. Chen⁷, E.S. Chen^{1,3}, G.H. Chen⁸, H.X. Chen¹³, Liang Chen¹⁴, Long Chen¹⁰, M.J. Chen^{1,3}, M.L. Chen^{1,3,11}, Q.H. Chen¹⁰, S. Chen¹⁵, S.H. Chen^{1,2,3}, S.Z. Chen^{1,3}, T.L. Chen¹⁶, X.B. Chen¹⁷, X.J. Chen¹⁰, Y. Chen¹⁷, N. Cheng^{1,3}, Y.D. Cheng^{1,2,3}, M.C. Chu¹⁸, M.Y. Cui¹², S.W. Cui¹⁹, X.H. Cui²⁰, Y.D. Cui²¹, B.Z. Dai¹⁵, H.L. Dai^{1,3,11}, Z.G. Dai⁴, Danzengluobu¹⁶, Y.X. Diao¹⁰, X.Q. Dong^{1,2,3}, K.K. Duan¹², J.H. Fan⁸, Y.Z. Fan¹², J. Fang¹⁵, J.H. Fang¹³, K. Fang^{1,3}, C.F. Feng²², H. Feng¹, L. Feng¹², S.H. Feng^{1,3}, X.T. Feng²², Y. Feng¹³, Y.L. Feng¹⁶, S. Gabici²³, B. Gao^{1,3}, C.D. Gao²², Q. Gao¹⁶, W. Gao^{1,3}, W.K. Gao^{1,2,3}, M.M. Ge¹⁵, T.T. Ge²¹, L.S. Geng^{1,3}, G. Giacinti⁷, G.H. Gong²⁴, Q.B. Gou^{1,3}, M.H. Gu^{1,3,11}, F.L. Guo¹⁴, J. Guo²⁴, X.L. Guo¹⁰, Y.Q. Guo^{1,3}, Y.Y. Guo¹², Y.A. Han²⁵, O.A. Hannuksela¹⁸, M. Hasan^{1,2,3}, H.H. He^{1,2,3}, H.N. He¹², J.Y. He¹², X.Y. He¹², Y. He¹⁰, S. Hernández-Cadena⁷, B.W. Hou^{1,2,3}, C. Hou^{1,3}, X. Hou²⁶, H.B. Hu^{1,2,3}, S.C. Hu^{1,3,27}, C. Huang¹⁷, D.H. Huang¹⁰, J.J. Huang^{1,2,3}, T.Q. Huang^{1,3}, W.J. Huang²¹, X.T. Huang²², X.Y. Huang¹², Y. Huang^{1,3,27}, Y.Y. Huang¹⁷, X.L. Ji^{1,3,11}, H.Y. Jia¹⁰, K. Jia²², H.B. Jiang^{1,3}, K. Jiang^{11,4}, X.W. Jiang^{1,3}, Z.J. Jiang¹⁵, M. Jin¹⁰, S. Kaci⁷, M.M. Kang²⁸, I. Karpikov⁹, D. Khangulyan^{1,3}, D. Kuleshov⁹, K. Kurinov⁹, B.B. Li¹⁹, Cheng Li^{11,4}, Cong Li^{1,3}, D. Li^{1,2,3}, F. Li^{1,3,11}, H.B. Li^{1,2,3}, H.C. Li^{1,3}, Jian Li⁴, Jie Li^{1,3,11}, K. Li^{1,3}, L. Li²⁹, R.L. Li¹², S.D. Li^{14,2}, T.Y. Li⁷, W.L. Li⁷, X.R. Li^{1,3}, Xin Li^{11,4}, Y. Li⁷, Y.Z. Li^{1,2,3}, Zhe Li^{1,3}, Zhuo Li³⁰, E.W. Liang³¹, Y.F. Liang³¹, S.J. Lin²¹, B. Liu¹², C. Liu^{1,3}, D. Liu²², D.B. Liu⁷, H. Liu¹⁰, H.D. Liu²⁵, J. Liu^{1,3}, J.L. Liu^{1,3}, J.R. Liu¹⁰, M.Y. Liu¹⁶, R.Y. Liu¹⁷, S.M. Liu¹⁰, W. Liu^{1,3}, X. Liu¹⁰, Y. Liu⁸, Y. Liu¹⁰, Y.N. Liu²⁴, Y.Q. Lou²⁴, Q. Luo²¹, Y. Luo⁷, H.K. Lv^{1,3}, B.Q. Ma^{25,30}, L.L. Ma^{1,3}, X.H. Ma^{1,3}, J.R. Mao²⁶, Z. Min^{1,3}, W. Mitthumsiri³², G.B. Mou³³, H.J. Mu²⁵, A. Neronov²³, K.C.Y. Ng¹⁸, M.Y. Ni¹², L. Nie¹⁰, L.J. Ou⁸, P. Pattarakijwanich³², Z.Y. Pei⁸, J.C. Qi^{1,2,3}, M.Y. Qi^{1,3}, J.J. Qin⁴, A. Raza^{1,2,3}, C.Y. Ren¹², D. Ruffolo³², A. Sáiz³², D. Semikoz²³, L. Shao¹⁹, O. Shchegolev^{9,34}, Y.Z. Shen¹⁷, X.D. Sheng^{1,3}, Z.D. Shi⁴, F.W. Shu²⁹, H.C. Song³⁰, Yu.V. Stenkin^{9,34}, V. Stepanov⁹, Y. Su¹², D.X. Sun^{4,12}, H. Sun²², Q.N. Sun^{1,3}, X.N. Sun³¹, Z.B. Sun³⁵, N.H. Tabasam²², J. Takata³⁶, P.H.T. Tam²¹, H.B. Tan¹⁷, Q.W. Tang²⁹, R. Tang⁷, Z.B. Tang^{11,4}, W.W. Tian^{2,20}, C.N. Tong¹⁷, L.H. Wan²¹, C. Wang³⁵, G.W. Wang⁴, H.G. Wang⁸, J.C. Wang²⁶, K. Wang³⁰, Kai Wang¹⁷, Kai Wang³⁶, L.P. Wang^{1,2,3}, L.Y. Wang^{1,3}, L.Y. Wang¹⁹, R. Wang²², W. Wang²¹, X.G. Wang³¹, X.J. Wang¹⁰, X.Y. Wang¹⁷, Y. Wang¹⁰, Y.D. Wang^{1,3}, Z.H. Wang²⁸, Z.X. Wang¹⁵, Zheng Wang^{1,3,11}, D.M. Wei¹², J.J. Wei¹², Y.J. Wei^{1,2,3}, T. Wen^{1,3}, S.S. Weng³³, C.Y. Wu^{1,3}, H.R. Wu^{1,3}, Q.W. Wu³⁶, S. Wu^{1,3}, X.F. Wu¹², Y.S. Wu⁴, S.Q. Xi^{1,3}, J. Xia^{4,12}, J.J. Xia¹⁰, G.M. Xiang^{14,2}, D.X. Xiao¹⁹, G. Xiao^{1,3}, Y.L. Xin¹⁰, Y. Xing¹⁴, D.R. Xiong²⁶, Z. Xiong^{1,2,3}, D.L. Xu⁷, R.F. Xu^{1,2,3}, R.X. Xu³⁰, W.L. Xu²⁸, L. Xue²², D.H. Yan¹⁵, T. Yan^{1,3}, C.W. Yang²⁸, C.Y. Yang²⁶, F.F. Yang^{1,3,11}, L.L. Yang²¹, M.J. Yang^{1,3}, R.Z. Yang⁴, W.X. Yang⁸, Z.H. Yang⁷, Z.G. Yao^{1,3}, X.A. Ye¹², L.Q. Yin^{1,3}, N. Yin²², X.H. You^{1,3}, Z.Y. You^{1,3}, Q. Yuan¹², H. Yue^{1,2,3}, H.D. Zeng¹², T.X. Zeng^{1,3,11}, W. Zeng¹⁵, X.T. Zeng²¹, M. Zha^{1,3}, B.B. Zhang¹⁷, B.T. Zhang^{1,3}, C. Zhang¹⁷, F. Zhang¹⁰, H. Zhang⁷, H.M. Zhang³¹, H.Y. Zhang¹⁵, J.L. Zhang²⁰, Li Zhang¹⁵, P.F. Zhang¹⁵, P.P. Zhang^{4,12}, R. Zhang¹², S.R. Zhang¹⁹, S.S. Zhang^{1,3}, W.Y. Zhang¹⁹, X. Zhang³³, X.P. Zhang^{1,3}, Yi Zhang^{1,12}, Yong Zhang^{1,3}, Z.P. Zhang⁴, J. Zhao^{1,3}, L. Zhao^{11,4}, L.Z. Zhao¹⁹, S.P. Zhao¹², X.H. Zhao²⁶, Z.H. Zhao⁴, F. Zheng³⁵, W.J. Zhong¹⁷, B. Zhou^{1,3}, H. Zhou⁷, J.N. Zhou¹⁴, M. Zhou²⁹, P. Zhou¹⁷, R. Zhou²⁸, X.X. Zhou^{1,2,3}, X.X. Zhou¹⁰,

B.Y. Zhu^{4,12}, C.G. Zhu²², F.R. Zhu¹⁰, H. Zhu²⁰, K.J. Zhu^{1,2,3,11}, Y.C. Zou³⁶, X. Zuo^{1,3},

POS (ICRC2025) 883

- ¹ Key Laboratory of Particle Astrophysics & Experimental Physics Division & Computing Center, Institute of High Energy Physics, Chinese Academy of Sciences, 100049 Beijing, China
- ² University of Chinese Academy of Sciences, 100049 Beijing, China
- ³ TIANFU Cosmic Ray Research Center, Chengdu, Sichuan, China
- ⁴ University of Science and Technology of China, 230026 Hefei, Anhui, China
- ⁵ Yerevan State University, 1 Alek Manukyan Street, Yerevan 0025, Armenia
- ⁶ Max-Planck-Institut for Nuclear Physics, P.O. Box 103980, 69029 Heidelberg, Germany
- ⁷ Tsung-Dao Lee Institute & School of Physics and Astronomy, Shanghai Jiao Tong University, 200240 Shanghai, China
- ⁸ Center for Astrophysics, Guangzhou University, 510006 Guangzhou, Guangdong, China
- ⁹ Institute for Nuclear Research of Russian Academy of Sciences, 117312 Moscow, Russia
- ¹⁰ School of Physical Science and Technology & School of Information Science and Technology, Southwest Jiaotong University, 610031 Chengdu, Sichuan, China
- ¹¹ State Key Laboratory of Particle Detection and Electronics, China
- ¹² Key Laboratory of Dark Matter and Space Astronomy & Key Laboratory of Radio Astronomy, Purple Mountain Observatory, Chinese Academy of Sciences, 210023 Nanjing, Jiangsu, China
- ¹³ Research Center for Astronomical Computing, Zhejiang Laboratory, 311121 Hangzhou, Zhejiang, China
- ¹⁴ Shanghai Astronomical Observatory, Chinese Academy of Sciences, 200030 Shanghai, China
- ¹⁵ School of Physics and Astronomy, Yunnan University, 650091 Kunming, Yunnan, China
- ¹⁶ Key Laboratory of Cosmic Rays (Tibet University), Ministry of Education, 850000 Lhasa, Tibet, China
- ¹⁷ School of Astronomy and Space Science, Nanjing University, 210023 Nanjing, Jiangsu, China
- ¹⁸ Department of Physics, The Chinese University of Hong Kong, Shatin, New Territories, Hong Kong, China
- ¹⁹ Hebei Normal University, 050024 Shijiazhuang, Hebei, China
- ²⁰ Key Laboratory of Radio Astronomy and Technology, National Astronomical Observatories, Chinese Academy of Sciences, 100101 Beijing, China
- ²¹ School of Physics and Astronomy (Zhuhai) & School of Physics (Guangzhou) & Sino-French Institute of Nuclear Engineering and Technology (Zhuhai), Sun Yat-sen University, 519000 Zhuhai & 510275 Guangzhou, Guangdong, China
- ²² Institute of Frontier and Interdisciplinary Science, Shandong University, 266237 Qingdao, Shandong, China
- ²³ APC, Université Paris Cité, CNRS/IN2P3, CEA/IRFU, Observatoire de Paris, 119 75205 Paris, France
- ²⁴ Department of Engineering Physics & Department of Physics & Department of Astronomy, Tsinghua University, 100084 Beijing, China
- ²⁵ School of Physics and Microelectronics, Zhengzhou University, 450001 Zhengzhou, Henan, China
- ²⁶ Yunnan Observatories, Chinese Academy of Sciences, 650216 Kunming, Yunnan, China
- ²⁷ China Center of Advanced Science and Technology, Beijing 100190, China
- ²⁸ College of Physics, Sichuan University, 610065 Chengdu, Sichuan, China
- ²⁹ Center for Relativistic Astrophysics and High Energy Physics, School of Physics and Materials

Science & Institute of Space Science and Technology, Nanchang University, 330031 Nanchang, Jiangxi, China

³⁰ School of Physics & Kavli Institute for Astronomy and Astrophysics, Peking University, 100871 Beijing, China

³¹ Guangxi Key Laboratory for Relativistic Astrophysics, School of Physical Science and Technology, Guangxi University, 530004 Nanning, Guangxi, China

³² Department of Physics, Faculty of Science, Mahidol University, Bangkok 10400, Thailand

³³ School of Physics and Technology, Nanjing Normal University, 210023 Nanjing, Jiangsu, China

³⁴ Moscow Institute of Physics and Technology, 141700 Moscow, Russia

³⁵ National Space Science Center, Chinese Academy of Sciences, 100190 Beijing, China

³⁶ School of Physics, Huazhong University of Science and Technology, Wuhan 430074, Hubei, China